Results in Engineering 30 (2026) 110786

Contents lists available at ScienceDirect

Results in Engineering

journal homepage: www.sciencedirect.com/journal/results-in-engineering

Bioplastic composite films from cellulose acetate and grape pomace for agricultural mulching: biodegradation and potential contribution to soil fertility

Nello Russo [a,†], Mirko Cucina [b,†], Maria Oliviero [a,*], Lucio Pisano [c], Piero Manna [c], Eugenia Monaco [c]

[a] Institute of Polymers, Composites and Biomaterials, National Research Council, P.le E. Fermi, 1, 80055 Portici, Italy
[b] National Research Council of Italy, Institute for Agricultural and Forest Systems in the Mediterranean, Via della Madonna Alta 128, 06128, Perugia, Italy
[c] National Research Council of Italy, Institute for Agricultural and Forest Systems in the Mediterranean, P.le E. Fermi, 1, 80055 Portici, Italy

ARTICLE INFO

Keywords:
Mulching film
Cellulose acetate
Grape pomace
Biodegradation
Soil

ABSTRACT

The accumulation of plastic waste from conventional agricultural mulching necessitates the development of sustainable, biodegradable alternatives. However, many biopolymers lack the necessary balance between durability during the crop cycle and efficient biodegradation. This study addressed this gap by adopting a *design-by-degradation* approach for the development of bioplastic composites based on thermoplastic cellulose acetate (CA) and grape pomace (GP) (from 10 to 50 wt%). To validate the engineering relevance of the materials, a multiscale characterization was performed, integrating mechanical tensile tests and surface wettability analysis with chemical (FT-IR), thermal (TGA, DSC), and morphological (SEM) assessments before and after 120 days of incubation in synthetic and agricultural soils.

Results demonstrate that the 30 wt% GP formulation represents the technical optimum: it maintains mechanical properties compatible with industrial requirements (Young's modulus ~900 MPa, tensile strength ~11 MPa, and elongation >10%), ensuring structural integrity during handling and service. Surface wettability analysis revealed that GP loading modulates initial hydrophilicity, facilitating microbial attachment, while a subsequent hydrophobic shift during degradation serves as a marker for plasticizer leaching and matrix deacetylation. While cumulative biodegradation increased with GP content, the degradation mechanism primarily involved enzymatic deacetylation and partial backbone cleavage, ensuring a programmable mechanical failure. Furthermore, bioplastic residues positively enhanced soil enzymatic activity in the short-term period analyzed, suggesting a beneficial role in nutrient cycling. This integrated methodology supports the transformation of standard biodegradation monitoring into a functional engineering protocol for optimizing the lifespan and sustainability of agricultural mulch films.

1. Introduction

Plastics, particularly films, play a crucial role in modern agriculture, with soil mulching representing one of their most widespread applications. Mulching films help regulate soil temperature, conserve moisture, and control weeds, thereby improving crop productivity [1]. However, the environmental impact of conventional plastic mulch films, especially their fragmentation and accumulation in soils, has raised increasing concern. Once incorporated into soil, plastic residues and microplastics can negatively affect soil structure, aeration, aggregate stability, and biochemical functioning [2,3]. In response to these concerns, biodegradable mulch films based on bioplastics have been increasingly proposed as alternatives to conventional polyethylene (PE) and polypropylene (PP) materials. These innovative materials offer several advantages in terms of environmental sustainability; however, their presence and degradation products may still induce changes in soil systems depending on environmental, soil, and climatic conditions [4]. In recent years, a growing number of studies have investigated their

* Corresponding author.
E-mail address: maria.oliviero@cnr.it (M. Oliviero).
† Authors contributed equally to work.

https://doi.org/10.1016/j.rineng.2026.110786
Received 15 December 2025; Received in revised form 9 March 2026; Accepted 28 April 2026
Available online 29 April 2026

biodegradability and potential impacts on soil ecosystems [5–7]. Biodegradability is one of the most important features of these materials, as it avoids long-term plastic accumulation in soils and eliminates the need for costly removal and disposal after use [8]. The biodegradation process involves a combination of biochemical and physico-chemical transformations, including enzymatic hydrolysis and mineralization to CO_2, as well as photooxidation and disintegration. These processes are strongly influenced by environmental factors such as temperature, soil type, water availability, microbial diversity, and the chemical composition of the bioplastic [9,10]. Overall, biodegradable plastics are expected to degrade within months to a few years, which is significantly faster than conventional fossil-based plastics [11,10].

Among the different bioplastics used in agriculture, blends of PLA (polylactic acid), PBAT (polybutylene adipate-co-terephthalate), PBSA (polybutylene succinate-co-adipate), and cellulose acetate (CA) derived from renewable sources such as cornstarch and plant biomass are widely investigated [12,13]. CA represents a promising matrix for biodegradable mulch films because it combines characteristics of natural polysaccharides and synthetic biopolyesters. Compared with other bioplastics such as PLA or PBAT, CA exhibits higher resistance to UV radiation and better thermal stability, ensuring the physical integrity of the mulch film during the crop cycle [14,15]. Derived from cellulose, the most abundant renewable polymer, CA also offers a high bio-based content [16,17]. Its functional properties, including gas permeability and moisture regulation, can be tuned by modifying the degree of substitution (DS), defined as the defined as the number of acetyl groups introduced per glucose monomer [18,19].

Cellulose acetate is produced through partial acetylation of cellulose, replacing hydroxyl groups with acetyl groups [20]. Secondary CA, characterized by an acetyl content of 53–56%, is suitable for thermoplastic processing. When the degree of substitution is $\leq$ 2.5, CA can undergo a synergistic biodegradation mechanism involving initial enzymatic deacetylation by esterases followed by cellulolytic degradation of the polymer backbone [21,22,19]. Furthermore, blending CA with easily degradable organic fillers derived from agricultural residues may enhance its biodegradability and reduce the persistence of plastic residues in soil. In this context, grape pomace (GP) represents a promising additive. As a major by-product of the wine industry, GP consists of skins, seeds, and stems and contains phenolic compounds, lipids, waxes, polysaccharides, and proteins [23]. Due to its large availability, GP valorization also has significant economic interest [24]. The incorporation of GP into biodegradable polymer matrices such as PLA, poly (butylene succinate), chitosan, and alginate has already been explored [25,26]. However, to the best of our knowledge, its incorporation into thermoplastic CA-based films has not yet been investigated. The addition of suitable plasticizers and organic fillers such as GP could allow the development of thermoplastic materials with adequate mechanical performance while promoting faster biodegradation in soil [27,28]. This effect is generally attributed to increased surface area, improved water absorption, and enhanced microbial colonization associated with the presence of organic fillers [29].

Despite the growing interest in biodegradable mulch films, important limitations remain. In particular, the development of thermoplastic CA mulch films incorporating GP has not yet been explored. Moreover, biodegradability is often assessed using standardized synthetic substrates (ISO 17556:2019), whereas studies conducted in real agricultural soils are still limited [9,30,31]. Synthetic substrates may overestimate biodegradation rates due to the high microbial activity typically associated with compost-rich media.

To address these gaps, this study adopted a *design-by-degradation* approach, where the engineering objective was to synchronize the functional lifespan of the material with the crop cycle. A multiscale characterization strategy was applied to CA–GP composites before and after soil incubation, including chemical (FT-IR), thermal (TGA, DSC), morphological (SEM), mechanical (tensile), and functional (wettability) analyses. By comparing degradation behavior in both synthetic and agricultural soils, the study aimed to optimize the formulation of the mulch film. Thus, the specific objectives were to (i) identify the most promising CA–GP composite formulation containing 10–50 wt% GP by evaluating its chemical, physical, and mechanical properties during biodegradation in different soils, and (ii) assess the preliminary effects of bioplastic residues on selected soil fertility indicators at the end of the incubation period.

2. Experimental section

2.1. Materials

2.1.1. Cellulose acetate

Pellets of plasticized cellulose acetate (CA), supplied by GIBAPLAST (Varese, Italy), were employed as the base matrix for the development of bioplastic composites. This commercial formulation, containing approximately 30 wt% plasticizer, was prepared using a cellulose acetate (degree of substitution (DS) = 2.5; 39.8 wt% acetyl content; Mn ~ 50,000) blended with triacetin (TA; 99.5% purity; Mw ~ 218.2 g/mol) and acetyl triethyl citrate (ATEC; 99% purity; Mw ~ 276.28 g/mol).

2.1.2. Grape pomace

Grape pomace (GP), obtained from the drying of Aglianico grape bunches grown in Irpinia (Montemiletto, AV) and kindly provided by ISAFOM-CNR (Institute for Agriculture and Forestry Systems in the Mediterranean – National Research Council of Italy), was used as filler component. GP was dried in an oven at 60 °C for 72 h and then milled using a 1 mm sieve grinding machine (CGOLDENWALL, Italy) at 500 rpm and sealed in zip lock paper bags until use. The main components of GP were water (50–70%), cellulose (10–20%), sugars (6–8%) fats (2–4%), organic acids (1–2%), tannins (1–2%) and minerals (1–2%) [32]. More details on content of cellulose, hemicellulose and lignin were reported in Table 1.

2.1.3. Bioplastic composites preparation

CA+GP bioplastic composites were prepared through a two-step process. The first step consists of melt blending the polymeric matrix CA with GP at different ratio (CA/GP = 90/10, 80/20, 70/30 and 50/50) by using an internal mixer (Rheomix® 600 Haake, Germany) controlled by a measuring drive (Haake Rheocord® 9000). The mixing chamber (volume of 50 cm^3) was filled with 50 g total mass. The rotation speed and mixing time were 50 rpm and 10 min for all tests. The mixing temperature was 150 °C. Before melting blending, all the components were pre-dried at 70 °C for 24 h. In the second step a P300P hot press (Collin, Germany) was used to prepare films with thickness of 1 mm. Materials were heated at the same temperature of mixing, pressed at 50 bar for 3 min and subsequently cooled to 30 °C under pressure. Pristine CA was subjected to the same procedure for proper comparison. The composition adopted for samples is reported in Table 2. The choice of melt mixing followed by compression moulding was intended to simulate the thermomechanical stress of industrial processing while

Table 1
Properties of grape pomace (modified from [33]).

Parameter	Value
pH	3.88 ± 0.02
EC (mS/cm)	4.2 ± 0.05
COD (mg O_2/g)[a]	1397 ± 50
C (%)[a]	48 ± 0.01
N (%)[a]	1.42 ± 0.01
O (%)[a]	34.6 ± 0.03
H (%)[a]	6.15 ± 0.02
Lignin (%)[a]	50.6 ± 1.40
Cellulose (%)[a]	19 ± 0.31
Hemicellulose (%)[a]	8.2 ± 0.02

[a] In dry basis.

Table 2
Composition of CA/GP composites (wt%).

Bioplastic Composites	CA (%)	GP (%)
CA	100	0
CA + 10% GP	90	10
CA + 20% GP	80	20
CA + 30% GP	70	30
CA + 50% GP	50	50

maintaining the sample thickness required by international standards for reliable characterizations. This batch-scale approach is widely documented in literature as a standard protocol for the preliminary validation of new bioplastic formulations and the assessment of their specific degradation mechanisms [34,20].

2.2. Biodegradation tests

Biodegradation tests were carried out following standardized incubation protocols (ISO 17556:2019) to ensure reproducibility and enable mechanistic interpretation of the effects of biodegradation on bioplastic composites, allowing the identification of the best composite for potential agricultural applications (i.e., balancing biodegradation and persistence). The duration of the incubation period (i.e., 120 days) was defined according to standardized incubation protocols and in accordance with the duration of horticultural crop cycles, which are commonly cultivated using mulching films.

2.2.1. Soils preparation

CA+GP bioplastic composites incubation in soil was performed with two different soils, i.e. synthetic soil (SS) and agricultural soil (SA). SS was prepared by mixing river sand (70% dry weight, dw, washed with deionized water, VWR International, Milano, Italy), natural soil (16% dw), clay (10% dw) compost (4% dw), KH_2PO_4 (0.2 g kg^{-1}, Merck KGaA, Darmstadt, Germany), $MgSO_4$ (0.1 g kg^{-1}, Merck KGaA, Darmstadt, Germany), $NaNO_3$ (0.4 g kg^{-1}, Merck KGaA, Darmstadt, Germany), $CO(NH_2)_2$ (0.2 g kg^{-1}, Merck KGaA, Darmstadt, Germany), and NH_4Cl (0.4 g kg^{-1}, Merck KGaA, Darmstadt, Germany) (ISO 17556:2019). SA was sampled (0–30 cm) from the same vineyard as the GP was produced, located in South Italy (Montemiletto, Campania region, 14,923,494 E, 41,016,659 N) after removing grass and roots. Soils characteristics (Table 3) were determined as follows: soil pH in aqueous solution using a 1:2.5 soil/water ratio (pH-Meter Basic 20+, Crison Instruments, Barcelona, Spain), total organic C (TOC) and total N (TN) by using an elemental analyzer (MacroCUBE CNHS, Elementar Italia, Lomazzo, Italy), and texture and water holding capacity (WHC) by using the Andreasen pipette and the Keen-Raczkowski Box, respectively. Before incubation, both soils were air-dried and sieved through a 2 mm particle size mesh and then adjusted with deionized water to bring the moisture to 50% of WHC. Prior to the beginning of the incubation, both soils prepared as described were preincubated in the dark at 23 °C in closed vessels for 7 days to ensure proper acclimatization.

Table 3
Main characteristics of synthetic and agricultural soil.

Parameter	Unit	Synthetic soil	Agricultural soil
Sand	%	70	42.5
Loam	%	14	19.7
Clay	%	16	37.8
Texture	-	Sandy loam	Clayey loam
Water holding capacity	%	14	25.6
pH	pH unit	6.6	8
Total organic C	%	2.3	1.1
Total N	%	0.2	0.2
C/N	-	11.5	5.5

Data are expressed on dry weigh basis.

2.2.2. Incubation in soils

Soil incubation of CA+GP bioplastic composites was carried out in hermetically closed 500 mL glass jars, under aerobic conditions following the standard method ISO 17556:2019 (i.e. incubation in the dark and at a controlled temperature of 23 °C for 120 days.). Soils without bioplastic composite addition (i.e. CTRL), positive reference (i.e. microcrystalline cellulose, CELL, Merck KGaA, Darmstadt, Germany) and negative reference (i.e. polypropylene, PP, Merck KGaA, Darmstadt, Germany) were included in the experimental setup, which resulted in 2 soils x (1 control + 2 references + 5 bioplastic composites) 8 thesis x 4 replicates = 64 glass jars. Pristine CA, CA+GP bioplastic composites and PP were reduced to squares of 1 cm x 1 cm prior to the beginning of the incubation (ISO 17556:2019). Each jar was filled with 200 g dw of the soil mixed with the tested material (concentration of 1.25% w/w) (ISO 17556:2019) and then closed. Soil moisture was maintained throughout the incubation period by weekly weighing the jars and adding deionized water to keep the weight of the jars constant.

During the incubation, soil respiration was monitored daily (in the first two weeks) and twice a week (starting from the third week) by measuring the CO_2 evolved from bioplastic composites biodegradation [31]. Briefly, CO_2 evolved was trapped in 2 M NaOH (2 mL) and titrated with 0.2 M HCl after precipitation of carbonates with 0.75 M $BaCl_2$ (phenolphthalein indicator). The results were expressed as % of bioplastic biodegradation calculated as the cumulative amount of C evolved from each sample divided by the amount of C of tested material and then multiplied by 100. Blank measurements (i.e. CTRL) were subtracted from each sample. Kinetic parameters of bioplastic composite biodegradation in soil were finally evaluated by using a non-linear first-order degradation model according to literature [35,36] (Eq. (1)):

$$B = B_0 \times \left[1 - e^{(-k \times t)}\right] \quad (1)$$

Where B is the biodegradation at time t, B_0 is the maximum biodegradation of the bioplastic, k ($days^{-1}$) is the kinetic constant, and t (days) is the time.

2.3. Characterization techniques

The morphological, thermal and chemical properties of the CA+GP based samples before and after biodegradation tests were studied using different characterization techniques, herein presented.

2.3.1. Elemental analysis and hydrophilicity

Elemental analysis of CA+GP based samples, as well as CELL and PP, was conducted through an elemental analyser (MacroCUBE CNHS, Elementar Italia, Lomazzo, Italy) to determine TOC and TN. C/N ratio was then calculated. Hydrophilicity of bioplastics and PP was determined by measuring the Water Uptake Capacity (WUC), as suggested by Papa et al. [31]. Briefly, about 0.1 g of sample was placed into a glass 100 mL flask filled with deionized water at 23 °C. After immersion for 24 h the samples were collected and gently treated with filter paper to remove all surface water. Then the wet samples were reweighed to determine the amount of water absorbed and WUC was calculated as in Papa et al. [31].

2.3.2. Scanning electron microscopy (SEM)

SEM Quanta 200 FEG (FEI, The Netherlands) was used to qualitatively check the surface morphology of the samples before and after degradation. Before placing the samples in the vacuum chamber, they were coated with a thin layer (about 10 nm thick) of an Au-Pd alloy by means of a sputter coating system (Emitech K575, Quorum Technologies LTD, UK). The images were captured using an acceleration voltage of 5 kV at a working distance of 6–9 mm.

2.3.3. Thermogravimetric analysis (TGA)

A thermogravimetric balance, TGA Q500 (TA Instruments, USA),

was used to analyze the thermal degradation behavior of the test samples between 30 °C and 800 °C at a heating rate of 10 °C/min in a nitrogen atmosphere.

2.3.4. Differential scanning colorimetry (DSC)

A DSC Discovery differential scanning calorimeter (TA Instruments, USA) was employed to determine the change in glass transition temperature (Tg) after the biodegradation process. The samples were weighed and analyzed under a nitrogen atmosphere at a heating rate of 10 °C/ min from - 50 to 200 °C.

2.3.5. Fourier transform infrared spectroscopy (FT-IR)

FT-IR analyses were performed using a Nicolet apparatus (Thermo Scientific, Italy) at ambient temperature. The samples were analysed in ATR spectra mode from 4000 to 600 cm^{-1} with a wavenumber resolution of 4 cm^{-1} for 64 scans.

2.3.6. Tensile tests

Tensile tests were performed at room temperature according to ASTM standard D882–12 by using a CMT 4304 Sans Testing Machine (SANS, Shenzhen, China) equipped with a 2.5 kN load cell. From stress vs elongation curve, the Young's modulus, stress and elongation at break were calculated. More specifically, the stress and strain at break were calculated at the last point of the stress-strain curve before failure, whereas the Young Modulus was evaluated based on the first linear region. For each sample, results were expressed as the average and standard deviation (SD) of five independent measurements.

2.3.7. Wettability analysis

The surface wettability of CA+GP composite films before and after biodegradation was evaluated by contact angle measurements of deionized water (WCA) by sessile drop method using an OCA 20 (Dataphysics, Filderstadt, Germany) goniometer, and data were collected with SCA 202 software (version 3.4.3 build 76). Equilibrium (static) contact angles were measured for 1 μL droplet volumes. Measurements were made in 10 different locations for each condition, and the average value was reported with the standard deviation.

2.4. Effects of bioplastic composites residues on agricultural soil quality

The effects of the residues of bioplastic composites on soil quality parameters were evaluated on the agricultural soil samples at 120 d (i.e. end of the experiments). To link bioplastic degradation with potential impacts on soil functioning, selected parameters were chosen to represent complementary indicators of soil quality, including chemical fertility (pH, total organic C, organic matter, total N, C/N ratio, and cation exchange capacity), microbial activity (soil respiration, microbial biomass C, metabolic quotient, and enzymatic activity), and physical properties (water holding capacity) relevant to agricultural performance. Chemical parameters were analyzed to evaluate changes in nutrient availability and carbon dynamics resulting from bioplastic residue incorporation, whilst biochemical indicators were measured to assess microbial responses and organic matter turnover associated with biodegradation processes. Finally physical indicators were included because polymer residues may influence soil structure and moisture retention. Together, these parameters provide an integrated assessment of how biodegradable mulching materials may affect soil fertility and ecosystem functioning, in line with the objectives of evaluating both biodegradation behavior and potential agronomic impacts. The selected parameters have been analyzed on air-dried soil samples, after proper homogenization (i.e. milling and sieving at 2 mm). CTRL, CELL, GP, and PP soil samples have also been included in the evaluation.

Soils characteristics were determined as follows and employing the methods described in Cucina et al. [37]. Soil pH was measured in aqueous solution using a 1:2.5 soil/water ratio (pH-Meter Basic 20+, Crison Instruments, Barcelona, Spain). TOC and TN were determined by using an elemental analyser (MacroCUBE CNHS, Elementar Italia, Lomazzo, Italy), and then organic matter and C/N ratio were calculated by multiplying TOC x 1.72 and dividing TOC/TN, respectively. Soil water holding capacity (WHC) was analyzed by the Keen-Raczkowski Box method, and cation exchange capacity (CEC) was determined by the magnesium sulphate method. Respiration rate and microbial biomass C were determined following the titration method reported in Section 2.2.2 and according to the fumigation-incubation method, respectively. Metabolic quotient was then calculated as the ratio between respiration rate and microbial biomass C. Finally, total enzymatic activity was determined according to the fluoresceine diacetate hydrolysis method.

2.5. Statistics

All data represent the arithmetic mean of four replicates, except where different reported in methods' description. Mean and standard deviation values were calculated using the Microsoft Excel Software. Determination of significant differences among the parameters analyzed over time at a level of significance of $P < 0.05$ was carried out by analysis of variance (ANOVA) and Tukey's test, after verifying the normality and the homoscedasticity of the data by graphical analysis of residuals (Microsoft Excel Solver 2013). Linear regression analysis was carried out to determine significant correlations between selected parameters at a level of significance of $P < 0.05$ (Microsoft Excel Solver 2013). Apparent kinetic constant (k) was calculated by adjusting experimental data (B, t) and using non-linear regression (Microsoft Excel Software).

3. Results and discussion

3.1. Bioplastics biodegradation in soil

3.1.1. Biodegradation in synthetic and agricultural soils

Results of bioplastics incubation in the two soils, i.e. synthetic and agricultural, are reported in Fig. 1. In SS, CELL was quickly biodegraded and the amount of C mineralized was higher than the 70% after only three weeks, proving that the synthetic substrate was properly prepared and able to test bioplastics biodegradation according to ISO 17556:2019 (Fig. 1A). Conversely, PP did not biodegrade during the incubation period, according to literature [38]. Cumulative biodegradation (%C) at 120 days for the bioplastics in SS decreased following the order: 61.8 ± 2.9% (CA+50%GP) > 55.1 ± 1.4% (CA+30%GP) > 37.4 ± 0.7% (CA+20%GP) > 33.5 ± 2% (CA) ≈ 33.2 ± 1% (CA+10%GP), showing significant differences among the tested materials ($P < 0.05$) with the exception of CA+10%GP, whose biodegradation was not different from pristine CA.

In SA, CELL biodegradation was slower and reached about 30% at the end of the incubation period (Fig. 1B). This is in accordance with literature, where CELL residence time in temperate soils is reported to range from about three to eighteen months [10]. PP did not show significant biodegradation in SA. Cumulative biodegradation (%C) of bioplastics in SA after 120 days showed the same trend as the one observed in SS, but lower values were measured: 34.8 ± 1.1% (CA+50%GP) > 31.9 ± 1.2% (CA+30%GP) > 21.8 ± 0.7% (CA+20%GP) > 18.2 ± 2.4% (CA) ≈ 17.5 ± 0.8% (CA+10%GP). Again, significant differences in biodegradation were observed for the tested materials ($P < 0.05$) apart from CA+10%GP, whose biodegradation was not different from pristine CA. Although statistically significant differences in biodegradation were observed among some materials, particularly at higher grape pomace contents, the magnitude of these differences was in certain cases relatively modest, especially for lower GP additions (e.g., CA vs CA+10% GP). Therefore, the results should primarily be interpreted in terms of overall trends rather than large performance differences between formulations. Literature reports contrasting results for CA and other bioplastics biodegradation in soil, and it was mainly explained because of

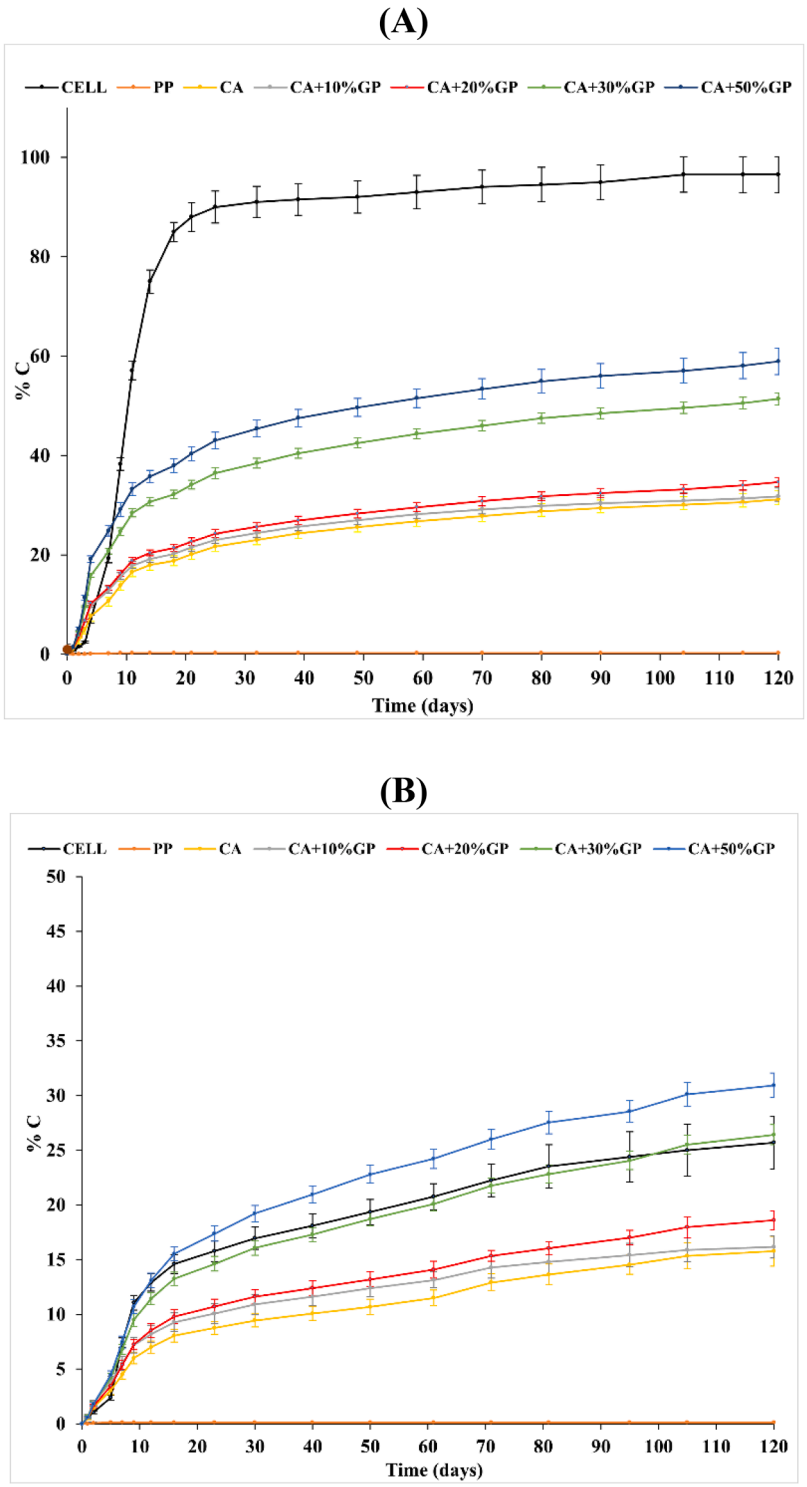

Fig. 1. Biodegradation of CELL, PP, CA and CA+GP samples in (A) SS and (B) SA. Error bars represent the standard deviation of the mean (n = 4)..

the variability in (i) bioplastics composition, (ii) environmental conditions (i.e. season, temperature, light exposition, precipitations), (iii) soil physico-chemical characteristic (i.e. moisture, texture, pH), and (iv) soil microbial community composition and activity [9,39]. For CA, it was proposed that biodegradation in soil may be the result of deacetylation and cleave of CA chains operated by different enzymes, highlighting the importance of a well-diversified microbial community to promote the degradation rate [39]. Indeed, biodegradation by cellulases can be inhibited by the acetyl-groups that offer protection against microbial attack, making the degree of substitution (DS) of CA a key parameter determining its biodegradation in soil [10]. Consequently, CA biodegradation in soil ranged from 5–10% to 100% in different studies conducted with CA characterized by different DS [40,41,30]. The results obtained in this study after 120 days of incubation of pristine CA in soil (i.e. about 33% and 18% of biodegradation in SS and SA, respectively) may thus be considered in accordance with literature. The higher values of biodegradation measured in SS with respect to SA might be the results of different concurring factors, being the soil microbial community composition and the water retention in soils the most important. SS was composed of 4% w/w of compost, which might have enriched the

synthetic substrate of microorganisms able to promote CA biodegradation through the enzymatic reactions above described. It is indeed reported that compost-sourced microorganisms can biodegrade CA quickly due to the production of esterases and cellulases [39]. Also, the water content and its availability in soil have a key role in bioplastics biodegradation [9]. In SA, CA biodegradation might have been slowed down due to the abundance of clays, which are characterized by a higher specific surface and water retention capacity with respect to sands (Table 3) [42].

3.1.2. Kinetic of biodegradation

From a kinetic perspective (Table 4), incorporating GP in CA promoted the biodegradation kinetic in all the GP concentrations tested in SA. Conversely, only blending 50% w/w of GP into CA increased biodegradation kinetic in SS (i.e. k increased from 0.055 to 0.071 day^{-1} from pristine CA to CA+50%GP). It may be hypothesized that in SA the effect of GP on biodegradation kinetic was more evident with respect to SS due to the slower biodegradation. Although the incorporation of grape pomace enhanced biodegradation kinetics and increased cumulative mineralization compared with pristine CA, the overall extent of mineralization in agricultural soil remained moderate after 120 days. This indicates that a substantial fraction of the material may persist in soil over the short-term, suggesting that GP incorporation accelerates initial degradation processes rather than ensuring rapid or complete residue removal. However, mineralization measured as CO_2 evolution represents only one pathway of carbon transformation in soil systems and does not fully describe the environmental fate of biodegradable polymer carbon. Recent work has highlighted that biodegradation in soils involves both respiratory carbon loss and microbial assimilation, with a substantial fraction of substrate carbon potentially incorporated into microbial biomass and soil organic matter pools [43,44]. Consequently, incomplete mineralization does not necessarily indicate environmental persistence, as non-mineralized carbon may be retained within biologically stabilized soil fractions. This perspective suggests that biodegradation should be interpreted within a broader carbon fate framework rather than solely as cumulative CO_2 production.

Although the incubation experiments were conducted under controlled laboratory conditions following standardized procedures, these conditions do not fully reproduce the complexity and variability of field environments where mulching films are applied. In agricultural settings, biodegradation rates may be strongly influenced by seasonal temperature fluctuations, wet–dry cycles, solar radiation exposure, soil heterogeneity, and spatial and temporal variability in microbial community composition and activity. Additional factors such as mechanical stress, plant–root interactions, and agricultural practices (e.g., tillage and irrigation) may further affect the fragmentation and degradation behavior of bioplastics [9]. The constant temperature, controlled moisture, and absence of environmental disturbances adopted in this study were intended to ensure reproducibility and allow comparison between materials and soil types; however, such conditions may either accelerate or limit degradation relative to field conditions. Therefore, the biodegradation rates reported here should be interpreted as indicative of intrinsic material behavior under standardized conditions rather than as direct predictions of field performance. Future studies should include long-term field trials and experiments under fluctuating environmental conditions to validate the environmental fate of CA–GP composites in real agricultural systems.

Table 4
First-order kinetic parameters of CA and CA+GP samples biodegradation in SS and SA.

	Synthetic soil			Agricultural soil		
Sample	B_o[a]	K[b]	R^2	B_o	k	R^2
CA	34	0.055	0.9752	18	0.019	0.9654
CA+10%GP	34	0.058	0.9778	18	0.027	0.9638
CA+20%GP	37	0.055	0.9678	22	0.025	0.9611
CA+30%GP	55	0.055	0.9686	32	0.023	0.9649
CA+50%GP	62	0.071	0.9781	35	0.025	0.9778

[a] Maximum biodegradation (%C).
[b] Kinetic constant of biodegradation ($days^{-1}$).

3.1.3. Effects of GP incorporation on CA biodegradation in soil

Interestingly, a positive effect of GP on CA soil biodegradation was observed in both studied soils. A significant positive correlation ($P < 0.001$) was indeed found between the cumulative biodegradation (%C) at 120 days and the amount of GP in the bioplastics (% w/w) in SS ($y = 2.3x - 34.6$, $r = 0.9423$, $n = 18$) and in SA ($y = 1.4x - 38.6$, $r = 0.9340$, $n = 18$). This was in accordance with literature, where the positive effects of easy-biodegradable additives to CA biodegradation were reported. For instance, the incorporation of polyethylene glycol prepared from *Parthenium hysterophorus* to CA enhanced the soil biodegradation of CA of about 30% in a 45-day incubation experiment (CA+50% w/w of polyethylene glycol) [30].

The positive effect of GP incorporation in CA bioplastics might be attributed to changes in the chemical and physical properties of the materials. First, incorporating GP in CA resulted in changes to the C/N ratio of the bioplastics, which decreased from 209 (CA) to 50.1 (CA+50%GP) (Table 5). Even though it remained much higher than microbial biomass C/N (about 5–10), the more balanced C/N ratio observed with increasing GP concentration may have favored the microbial biodegradation of bioplastics, as confirmed by the significant negative correlation ($P < 0.05$) found between the cumulative biodegradation (%C) at 120 days and the C/N ratio of bioplastics in SS ($y = -3.1x + 242$, $r = 0.6444$, $n = 18$) and in SA ($y = -5.4x + 242$, $r = 0.6968$, $n = 18$). Taking all this into consideration, decreasing the C/N ratio of the bioplastic composite, i.e., using a filler with higher N content, could be a useful strategy to promote composite biodegradation and reduce the risk of soil N immobilization, which is commonly reported in field experiments due to the unbalanced C/N ratio of soils treated with plastics and bioplastics [45].

Apart from the C/N ratio, hydrophilicity of bioplastics (i.e. as estimated by WUC, Table 5) was found to be a major driver of bioplastics biodegradation in soil and this was expected since most of the enzymatic reactions involved in bioplastics biodegradation are water-mediated [9]. WUC of bioplastics was related to the amount of GP incorporated in CA mainly because of the hydrophilic characteristics of the carbohydrates and fibers constituting GP [23]. WUC was found to be positively correlated ($P < 0.001$) with the cumulative biodegradation of bioplastics in soil ($y = 0.48x - 13.2$, $r = 0.9267$, $n = 18$, SS; $y = 0.81x - 11.8$, $r = 0.9370$, $n = 18$, SA), showing a more significant effect on bioplastics biodegradation with respect to the C/N ratio of the bioplastics. This was in accordance with Papa et al. [31] who showed that hydrophilicity of aged PLA and starch-based bioplastic was the main driver of their biodegradation for 120-day incubation in a synthetic soil.

Table 5
Total organic C, total N, C/N and wettability of CELL, PP, CA and CA+GP samples.

Sample	Total organic C (%)	Total N (%)	C/N	WUC[a] (%)
CELL	43.4 ± 0.9[b]	0.02 ± 0.04	2170	n.d.[c]
PP	84 ± 0.8	3.8 ± 1.1	22.1	0.18 ± 0.22
CA	50.3 ± 0.5	0.24 ± 0.15	209	4.2 ± 0.9
CA+10%GP	50 ± 0.1	0.43 ± 0.19	116	7.8 ± 0.2
CA+20%GP	51.5 ± 1	0.74 ± 0	69.6	11.2 ± 0.7
CA+30%GP	51.3 ± 1	0.61 ± 0.02	84.1	14.2 ± 0.9
CA+50%GP	50.1 ± 0.3	1 ± 0	50.1	18.2 ± 1.3

Data are expressed on dry weigh basis;.
[a] Water uptake capacity (ISO 62:2008);.
[b] Mean value ± Standard Deviation, n = 4.
[c] Not determined.

3.2. Morphological, thermal and chemical modifications induced by biodegradation

3.2.1. SEM analysis

SEM analysis (Fig. 2) revealed a fundamental divergence in the degradation behaviour of pristine CA compared to the CA+50%GP composite. Initially, the smooth, homogeneous surface of the pristine matrix contrasted with the inherently rough topography of the composite (Fig. 2a), where the presence of the filler increased the effective surface area and provided preferential sites for microbial colonization. After 120 days of incubation, pristine CA exhibited only superficial erosion, whereas the CA+50%GP samples underwent pronounced structural deterioration. In SS, the composite showed extensive exfoliation, deep cavities, and macro-fractures (Fig. 2b). These morphological alterations were consistent with the high mineralization degree (61.8 ± 2.9%) and the rapid degradation kinetics (k = 0.071 day^{-1}) reported in Table 4. Although the SA environment was significantly less aggressive than SS, the CA+50%GP composite still demonstrated a markedly greater extent of degradation compared to pristine CA (Fig. 2c). This disparity confirmed that, even under less favourable microbial conditions, the incorporation of GP acted as a key driver for initiating surface erosion and accelerating structural decay. Overall, while the GP filler was crucial for triggering and enhancing the biodegradation of the CA matrix [46], the cracking observed at 50% loading [20] highlighted a critical trade-off: while the filler effectively accelerated microbial breakdown, it simultaneously compromised structural integrity by inducing severe embrittlement. Consequently, while the 50% GP formulation ensures rapid end-of-life breakdown, its premature loss of physical cohesion suggests that lower filler loadings might be more suitable for maintaining the functional integrity required during the active phase of mulching.

3.2.2. TGA and DSC insights

The thermal degradation profiles and associated parameters for

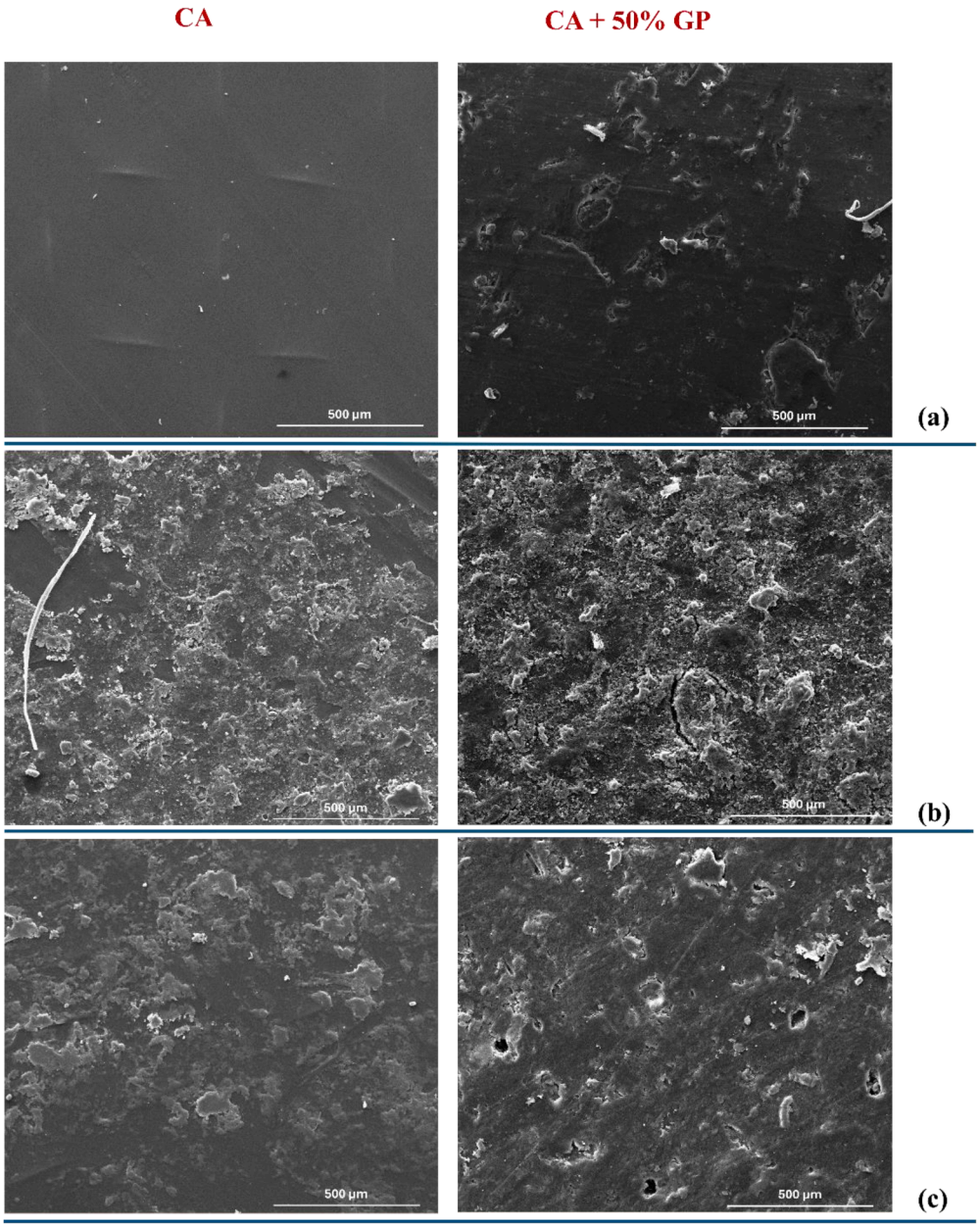

Fig. 2. SEM images at 500µm of CA and CA + 50% GP samples: (a) before biodegradation; (b) post 120 days of incubation in SS; (c) post 120 days of incubation in SA.

pristine CA and its composites are presented in Fig. 3 and Table 6.

Prior to incubation, all samples exhibited a three-stage weight loss: the first two stages were attributed to the evaporation of TA and ATEC plasticizers, while the third corresponded to the thermal pyrolysis of the cellulose acetate backbone [47]. Notably, the evaporation temperatures for TA and ATEC exceeded their respective pure boiling points (190 °C and 230 °C), suggesting restricted molecular diffusion and strong interactions within the CA matrix [48–50]. The incorporation of GP slightly increased the initial moisture content due to its hydrophilic nature [23] and lowered both the onset degradation temperature (T_I) and the temperature of maximum degradation rate (T_{max}), indicating a catalytic effect of the filler on matrix decomposition [26].

Post-incubation analysis revealed profound structural alterations, most notably the complete disappearance of the mass loss steps associated with TA and ATEC in composites containing >10 wt.%. This confirmed extensive plasticizer leaching during soil exposure, directly explaining the observed embrittlement. While pristine CA exhibited a downward shift in both T_I and Tmax, consistent with network weakening, the bioplastic composites showed a different behaviour: a decrease in T_I accompanied by an increase in Tmax. This suggested that plasticizer removal results in a polymer framework that was less stable at the degradation onset but more resistant at the maximum decomposition stage due to increased rigidity.

The glass transition behaviour (Tg), analyzed by DSC (Fig. 4), further supported this structural evolution. Initially, GP restricted chain mobility, shifting Tg to higher temperatures [34,26]. Although biodegradation commonly lowers Tg through molecular weight reduction [51], an increase in Tg was observed after incubation in both SS and SA. For composites containing >20 wt.% GP, Tg became undetectable within the explored thermal range. This behaviour indicated that leaching and progressive deacetylation occurred simultaneously, promoting enhanced intermolecular hydrogen bonding and partial restoration of the cellulose supramolecular architecture [20]. This restructuring, more pronounced in the aggressive SS environment, confirms that the material undergoes a fundamental chemical transition that facilitates its eventual assimilation by the soil microbiota.

Table 6
TGA and DSC results of pristine CA and composites CA+GP before and after 120 days of incubation in SS and SA, respectively.

Sample	T_{TA} (°C)	T_{ATEC} (°C)	T_I (°C)	T_{max} (°C)	Tg (°C)
GP	-	-	205	270	-
CA	220	285	319	365	112
CA +10% GP	221	274	293	342	117
CA +20% GP	241	272	291	333	119
CA +30% GP	249	271	291	322	121
CA +50% GP	240	271	290	313	130
CA_SS	-	282	298	348	139
CA +10% GP_SS	-	274	287	344	190
CA +20% GP_SS	-	-	290	342	ND
CA +30% GP_SS	-	-	288	345	ND
CA +50% GP_SS	-	-	280	342	ND
CA_SA	-	292	318	364	134
CA +10% GP_SA	-	270	283	350	181
CA +20% GP_SA	-	-	290	359	ND
CA +30% GP_SA	-	-	290	353	ND
CA +50% GP_SA	-	-	289	359	ND

3.2.3. FT-IR analysis

The chemical modifications induced by microbial degradation on the surface of test samples were investigated by ATR FT-IR. Fig. 5a, b and c show ATR spectra of pristine CA and all bioplastic composites before and after 120 days of incubation in SS and SA, respectively. In Fig. 5a the ATR spectrum of GP is also reported as a reference. For pristine CA before degradation, the peak at 3485 cm^{-1} can be attributed to the O—H bond stretching of unacetylated cellulose and the peak at 2952 cm^{-1} is for C—H stretching of methyl groups (–CH_3). The characteristic peak at 1734 cm^{-1} is assigned for carbonyl stretch of the acetate function and the peak at 1642 cm^{-1} is correlated to H—O-H bending of absorbed water. Peaks at 1435 cm^{-1}, 1371 cm^{-1}, 1215 cm^{-1}, 1030 cm^{-1} and 904 cm^{-1} can be ascribed to CH_2 bending, C—H bending vibration of CH_3 in the acetyl group, C–O stretching of acetyl group, C–O–C stretching of cellulose backbone and C—O-C stretching at β–(1 → 4) glycosidic linkage, respectively [52]. The contribution of plasticizers (TA and ATEC) was also considered, as they share functional groups with cellulose acetate. Changes in peak intensity and position were evaluated relative to pure CA. No significant changes in the peaks were observed after the addition of GP, likely due to its uniform distribution in the matrix and overlap of GP bands with CA peaks [53]. After 120 days of incubation in SS and SA, the spectra of pristine CA showed only minor variations. A decrease in absorbance at 1734, 1371, 1215, 1030 and 904 cm^{-1}, along with the broadening and shift and of the hydroxyl band at 3485 cm^{-1}, indicated plasticizers loss, partial deacetylation and some degradation of cellulose backbone [20]. In contrast, CA+GP samples exhibited pronounced spectral changes after 120 days in both soils. The band at 1734 cm^{-1} decreased markedly and became undetectable at higher GP contents, reflecting complete plasticizers loss and extensive deacetylation. The hydroxyl band at 3485 cm^{-1} increased in intensity, while the peak at 904 cm^{-1} decreased and eventually disappeared with increasing GP, indicating significant backbone degradation. Additionally, all spectra displayed an increased absorbance at 1642 cm^{-1}, associated with water uptake during degradation, and the appearance of a peak at 1550 cm^{-1}, indicative of proteinaceous compounds most likely produced by bacterial activity [54]. The absence of an invariant peak in both spectra prevented a reliable semi-quantitative evaluation via normalization or internal standard methods. Indeed, the concurrent leaching of plasticizers and the extensive deacetylation of the polymer backbone, as evidenced by the drastic reduction or disappearance of peaks at 1734 and 904 cm^{-1} and corroborated by TGA results showing complete plasticizer loss for GP content exceeding 10 wt% (Table 6), altered all potential reference bands. Consequently, the analysis was restricted to

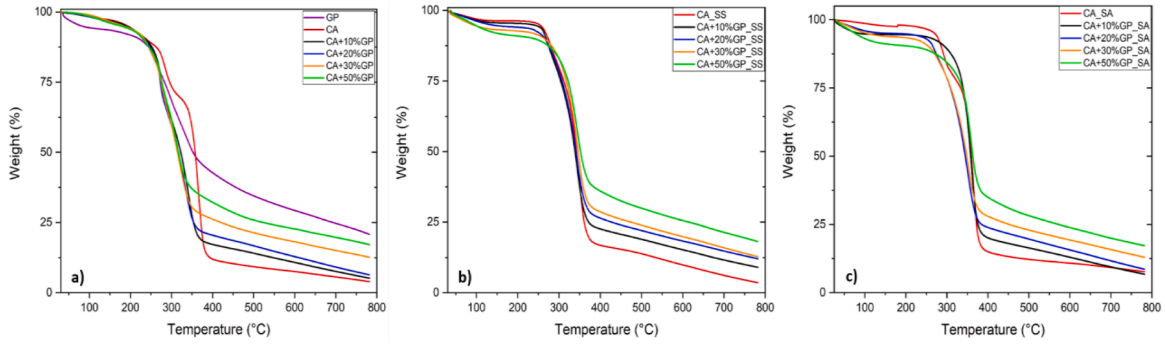

Fig. 3. TGA profiles of pristine CA and composites CA-GP (a) before and after 120 days of incubation in (b) SS and (c) SA, respectively.

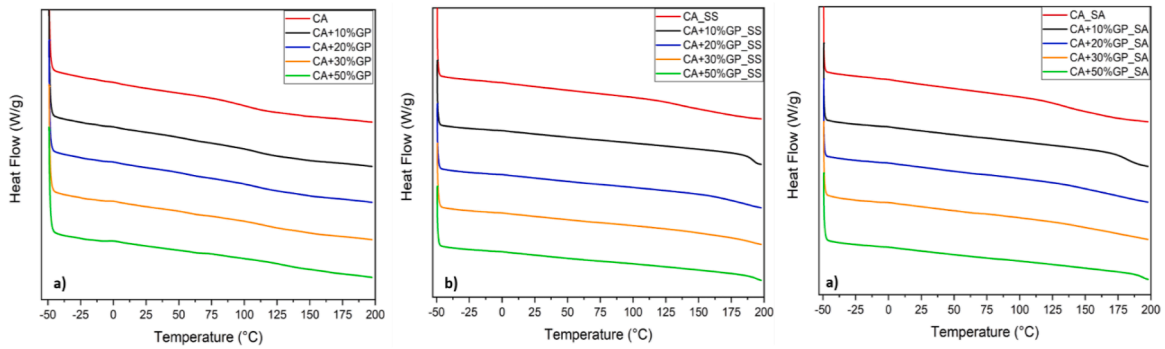

Fig. 4. DSC curves of pristine CA and composites CA-GP (a) before and after 120 days of incubation in (b) SS and (c) SA, respectively.

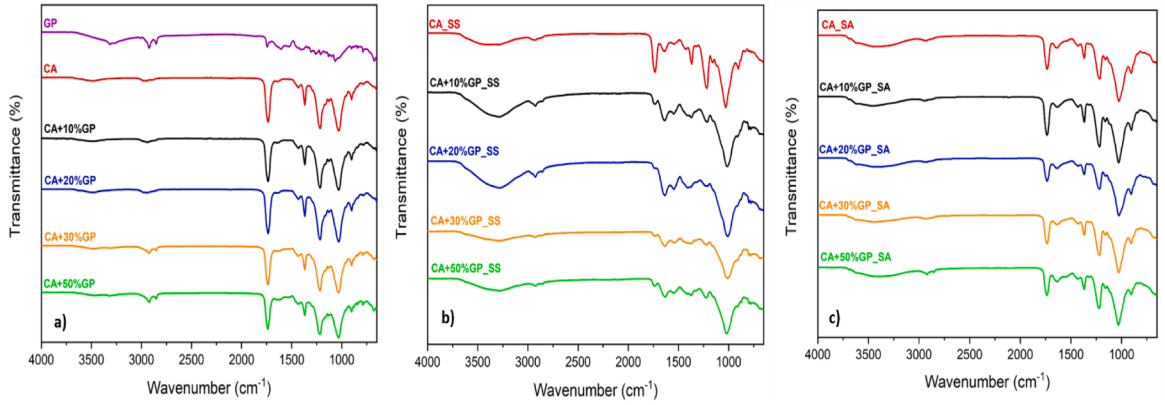

Fig. 5. FTIR spectra of pristine CA and composites CA-GP (a) before and after 120 days of incubation in (b) SS and (c) SA, respectively.

qualitative observations of the spectral variations to avoid the introduction of quantitative artefacts. These spectra changes confirm that both deacetylation and degradation were enhanced by SS and by the presence of GP, in agreement with previous literature [55,39]. In addition, the spectroscopic variations confirm that the filler loading directly modulates the intensity of these chemical modifications, governing the structural transition of the matrix during soil exposure. The degradation mechanism involves an initial deacetylation step, concomitant with plasticizer leaching, followed by chain scission of the "regenerated" cellulose backbone, ultimately leading to material embrittlement and the formation of sugars as final degradation products [19].

3.2.4. *Mechanical properties*

The incorporation of GP induced a concurrent decline in stiffness, strength, and ductility (Table 7). Specifically, the Young's modulus and stress at break decreased to 900 MPa and 10.9 MPa respectively at 30 wt % of GP, while the elongation at break dropped to 14%. These trends are attributed to the filler particles acting as structural discontinuities and stress concentrators that interrupt the polymer network, simultaneously reducing the resistance to elastic deformation and restricting the mobility of the polymer chains [56]. Despite this overall downward trend, the composites CA+GP maintain a performance profile compatible with agricultural requirements. The Young's modulus and tensile strength values meet the standard requirements for agricultural films (200–1000 MPa for stiffness and 10–14 MPa for strength). This ensures that the material is robust enough to withstand mechanical installation and environmental stress without deforming or breaking [57,58]. Similarly, although the filler-induced embrittlement is evident, the elongation at break for the 30% GP formulation stays above the critical safety threshold of 10%, which is essential to prevent tearing and brittle failure during field handling [57]. The system reaches a critical instability at 50 wt% GP loading, where the insufficient matrix volume fails to encapsulate the filler, leading to film fragmentation [59]. After 120 days of soil incubation in SS and SA, the combined effect of plasticizer leaching, enzymatic deacetylation, and partial backbone biodegradation led to a severe embrittlement of the composites. This loss of molecular flexibility rendered the samples too fragile for post-degradation mechanical characterization. Ultimately, a filler content (10–30 wt%) successfully modulates the material's life-cycle by ensuring necessary tenacity during service while enabling a controlled mechanical failure once applied to the soil [60].

Table 7
Mechanical properties of pristine CA and composites CA+GP before incubation.

Bioplastic Composites	Young's modulus (MPa)	Stress at break (MPa)	Elogation at break (%)
CA	1108 ± 59	15.8 ± 1.4	20 ± 3.1
CA + 10% GP	1049 ± 23	13.7 ± 1.9	18 ± 1.0
CA + 20% GP	978 ± 18	12.5 ± 2.0	16 ± 1.8
CA + 30% GP	900 ± 31	10.9 ± 0.9	14 ± 2.1

3.2.5. *Surface wettability*

Surface wettability (Fig. 6) serves as a decisive functional parameter for agricultural mulch films, as it regulates the material's interaction with irrigation water and soil moisture, thereby governing the overall biodegradation kinetics. At the onset of the study (Day 0), the pristine CA film exhibited a static water contact angle (θ) of approximately 70° The introduction of 10 wt% GP significantly enhanced surface hydrophilicity, with θ dropping to 49° (Figs. 6a and b); this shift is primarily attributed to the exposure of polar hydroxyl groups inherent to the

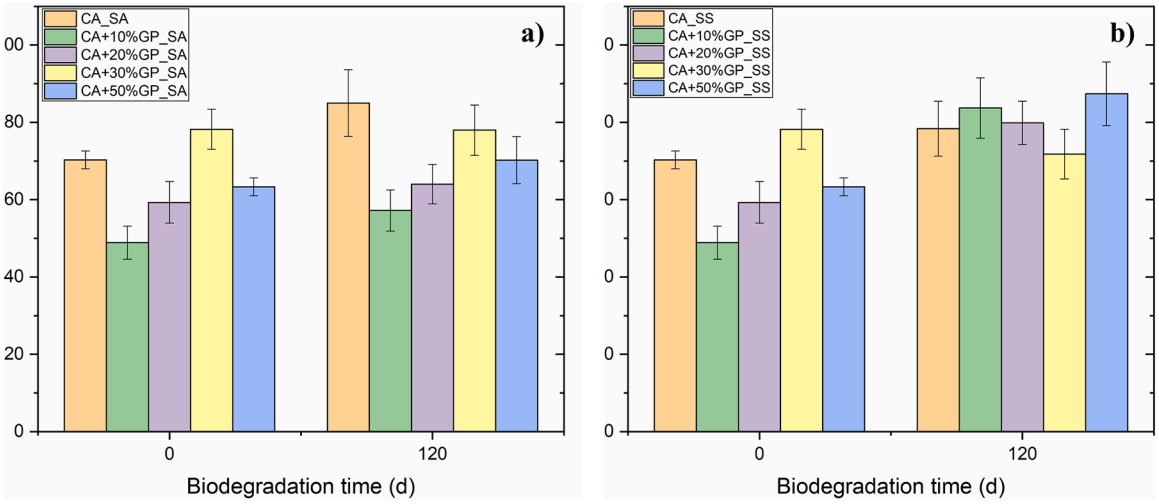

Fig. 6. Water Contact Angle before and after 120 days of incubation in (a) SS and (b) SA, respectively.

lignocellulosic structure of the GP [61,56]. However, as filler content increased further (20–50 wt%), the contact angle stabilized between 60° and 64°, suggesting that the increased surface micro-roughness at higher concentrations begins to partially offset the hydrophilic contribution of the GP particles, a phenomenon characteristic of biocomposites with heterogeneous surface morphologies [59]. The long-term evolution of these surfaces over 120 days of soil incubation revealed a significant "hydrophobic shift." Contrary to the typical expectation that degradation increases hydrophilicity through surface oxidation, the contact angles in this study rose across almost all formulations, with the magnitude of this change being distinctly modulated by the soil type. In the SS, the hydrophobic shift was most pronounced, particularly for the CA+50%GP sample which reached a peak of nearly 87° (Fig. 6a). This trend indicates that the intense microbial activity in the SS quickly consumes the most bioavailable components, leaving behind a highly irregular and crystalline surface residue. Conversely, the SA promoted a more gradual evolution; while the pristine CA rose to 84°, the composites with 10% and 20% GP maintained lower angles than their SS counterparts (Fig. 6b), suggesting that the SA medium facilitates a more controlled and slower surface erosion. Across both environments, this overall increase in θ serves as a macroscopic marker for the underlying degradation mechanism driven by the leaching of hydrophilic plasticizers and the preferential microbial consumption of the amorphous regions within the CA matrix [19,60]. As these bioavailable components are depleted, the surface becomes enriched with chemically stable crystalline residues and develops a degraded, micro-rough morphology that effectively hinders water spreading [57,62]. Synthesizing these observations, the 30 wt% GP formulation emerges as the technical optimum for agricultural applications. While the 50 wt% loading shows high initial reactivity, its sharp hydrophobic shift in SS environments signals a rapid loss of structural integrity and excessive brittleness [59]. The 30 wt% loading, however, provides the most balanced performance by ensuring a sufficiently hydrophilic surface at the start (θ~ 61°) to facilitate early microbial attachment, while maintaining a stable wettability profile that preserves mechanical performance for a full crop cycle [57]. Consequently, this formulation enables a "programmable" degradation profile, ensuring the film remains functional during service before transitioning into an accessible carbon source for soil microorganisms once its primary task is complete.

3.3. *Preliminary evaluation of the effects of bioplastic composites residues on soil fertility*

The preliminary evaluation of the effects of bioplastics composites residues on soil fertility indicators was carried out on agricultural soil samples at 120 days of incubation. The same evaluations on the synthetic soil samples were considered not relevant. To facilitate interpretation of soil responses, the results are discussed by distinguishing between short-term effects associated with the incorporation of biodegradable materials and longer-term effects related to material persistence in soil. Short-term responses mainly include changes in microbial activity, respiration, and labile organic matter dynamics resulting from the rapid utilization of easily degradable substrates. In contrast, longer-term effects are associated with the persistence of residual polymer fractions and their gradual mineralization, which may influence soil organic matter dynamics and fertility over extended periods. This distinction is particularly relevant under controlled incubation conditions, where the experimental timeframe captures early biodegradation stages rather than the complete environmental fate of the materials. After 120 days of incubation, significant differences in soil fertility parameters were observed among treatments for SA samples (Table 8). Soil pH remained near neutral across treatments, although pristine CA and its composites with GP slightly increased pH values compared to the control (CTRL), reaching up to 7.6 in CA+30%GP. Cellulose biodegradation in soil can increase soil pH because microbial decomposition consumes protons, releases ammonium-N, and reduces the effect of acidic cations. These processes may collectively shift soil conditions toward alkalinity. TOC was strongly affected by the treatments, and these changes may reflect both short-term substrate inputs and the persistence of less degradable material fractions. CA-amended soils exhibited the highest TOC (1.89%), significantly higher than CTRL (1.33%) and PP (1.35%), while GP alone did not significantly increase TOC, probably because of its quick mineralization in soil (Fig. 1, Table 4). Interestingly, when GP was incorporated into CA, TOC values remained elevated, especially at 10 and 20% GP addition (1.79% and 1.84%, respectively), before decreasing at higher GP proportions. This suggests that the presence of undegraded CA residues may provide a persistent carbon pool contributing to soil C stocks. Confirming this latter hypothesis, the extent of biodegradation of bioplastics in the soil at 120 days was found to be negatively correlated to the TOC ($y = -0.01x+2$, $r = 0.8743$, $n = 18$, $P < 0.05$). Similarly, organic matter content was significantly higher in CA-amended soils, indicating a sustained input of recalcitrant organic substrates. TN content showed no significant differences among treatments, with values ranging from 0.14 to 0.21%. The limited variation suggests minimal short-term impact within the experimental timeframe. Consequently, C/N ratios varied, with CELL and CA treatments displaying significantly higher values (>11) compared to CTRL and GP. Such increases reflect the addition of carbon-rich, nitrogen-poor substrates, which could influence microbial demand for available N [63].

Table 8
Effects of the biodegradable mulching films residues on the main fertility parameters of the agricultural soil (120 days) (Mean value ± SD, n = 4).

Parameter	Unit	CTRL	CELL	GP	PP	CA	CA+10% GP	CA+20% GP	CA+30% GP	CA+50% GP
pH	-	6.9 ± 0.1a	7 ± 0.1a	7 ± 0.1a	6.9 ± 0.1a	7.3 ± 0.1b	7.4 ± 0b	7.4 ± 0b	7.6 ± 0.2b	7.5 ± 0b
Total organic C	%	1.33 ± 0.19a	1.63 ± 0.03b	1.4 ± 0.15a	1.35 ± 0.04a	1.89 ± 0.12c	1.84 ± 0.08c	1.79 ± 0.03c	1.78 ± 0.2c	1.64 ± 0.02b
Organic matter	%	2.3 ± 0a	2.8 ± 0.1b	2.4 ± 0.1a	2.3 ± 0.2a	3.3 ± 0c	3 0.2 ± 0.1c	3.1 ± 0.2c	3.1 ± 0c	2.8 ± 0.1b
Total N	%	0.17 ± 0.03	0.14 ± 0.03	0.21 ± 0.03	0.17± 0.01	0.16 ± 0.02	0.16 ± 0.02	0.15 ± 0.03	0.18 ± 0.02	0.17 ± 0.17
C/N	-	7.8 ± 0.5a	11.6 ± 1.9b	6.7 ± 0.6a	7.9 ± 0.6a	11.8 ± 1.2b	11.5 ± 0.4b	9.9 ± 0.8b	9.9 ± 0.8b	9.6 ± 0.3b
Cation exchange capacity	meq 100 g^{-1}	32 ± 2a	31 ± 3a	33 ± 3a	39 ± 3b	38 ± 1b	38 ± 1b	39 ± 1b	37 ± 1b	37 ± 1b
Water holding capacity	%	41 ± 1a	41 ± 1a	38 ± 3a	40 ± 1a	48 ± 0b	47 ± 1b	51 ± 3b	50 ± 2b	49 ± 3b
Respiration rate	mgC-CO_2 kg^{-1} D^{-1}	6.1 ± 0.2a	15.7 ± 0.8c	11.3 ± 0.3b	6.3 ± 0.2a	11.8 ± 0.5b	11.6 ± 0b	12.8 ± 0.6b	13 ± 1b	12.9 ± 0.4b
Microbial biomass C	mgC kg^{-1}	1056 ± 29b	1280 ± 110c	1487 ± 94c	843 ± 51a	1416 ± 100c	1498 ± 87c	1678 ± 28d	1452 ± 45c	1305 ± 55c
Metabolic quotient	mgC-CO_2 mgC^{-1} D^{-1}	0.006 ± 0.003	0.012 ± 0.004	0.008 ± 0.002	0.007 ± 0.002	0.008 ± 0.001	0.008 ± 0.003	0.008 ± 0	0.009 ± 0.002	0.009 ± 0.002
Total enzymatic activity	mgFluoresceine kg^{-1} h^{-1}	161 ± 10a	202 ± 18b	235 ± 9b	158 ± 3a	222 ± 21a	247 ± 12b	228 ± 8b	219 ± 21b	219 ± 5b

Data are expressed on dry mass. Different letters in a row indicate significant differences among treatment at $P < 0.05$.
CTRL: control, CELL: cellulose, GP: grape pomace, PP: polypropylene, CA: cellulose acetate, CA+10%GP: cellulose acetate + 10% grape pomace, CA+20%GP: cellulose acetate + 20% grape pomace, CA+30%GP: cellulose acetate + 30% grape pomace, CA+50%GP: cellulose acetate + 50% grape pomace.

Cation exchange capacity (CEC) was slightly but significantly enhanced in PP- and CA-amended soils (up to 39 meq 100 g^{-1}), compared to CTRL (32 meq 100 g^{-1}). This suggests that organic inputs from polymers, also synthetic, and pomace may have contributed additional exchange sites, potentially improving soil nutrient retention. These results were in contrast with findings of Celletti et al. [64], who observed that the addition of starch-based bioplastics reduced the CEC of the soil employed. Nevertheless, in the study of Celletti et al. [64], the soil employed was a cultivation substrate and the results should be thus carefully compared, highlighting the need for testing bioplastics in real soils. Similarly, WHC was notably higher in CA and CA+GP treatments (up to 50%), highlighting the capacity of these residues to increase soil moisture retention. Such effects are ecologically relevant, as improved WHC can enhance resilience to drought stress.

With respect to biochemical fertility indicators, microbial respiration rates were significantly elevated in soils amended with CELL (15.7 mg C—CO_2 kg^{-1} d^{-1}) and CA+GP mixtures (from 11.6 to 13 mg C—CO_2 kg^{-1} d^{-1}), compared to CTRL (6.1 mg C—CO_2 kg^{-1} d^{-1}). These findings indicate that bioplastic residues can stimulate microbial catabolic activity in the short-term, possibly by providing semi-recalcitrant carbon sources. Indeed, the labile organic components have likely been mineralized during incubation. PP, in contrast, did not enhance microbial respiration, confirming its recalcitrant and biologically inert nature. MBC also responded positively to the presence of bioplastics residues, with the highest values observed for CA+20%GP (1678 mgC kg^{-1}), nearly 60% higher than CTRL (1056 mg C kg^{-1}). Remarkably, soils containing undegraded CA residues consistently supported higher MBC than the positive control CELL, suggesting that CA provides a C pool capable of sustaining microbial growth. Conversely, PP significantly reduced microbial biomass (843 mg C kg^{-1}), indicating a negative impact on microbial growth and activity. This highlights a stark difference between inert, petroleum-based plastics and partially degradable bioplastics, with the former potentially exerting detrimental effects on microbial functioning. These results are in accordance with Mazzon et al. [45] who reported significant effects of 1% w/w biodegradable starch-based bioplastic mulching film on the growth of soil microbial biomass, as well as increased carbon mineralization. Metabolic quotient, expressing the ratio between the respiration rate and the amount of microbial biomass, represents a useful proxy of the microbial activity and stress, i.e. an increased metabolic quotient is often associated with environmental stress for the microbial community [65]. In this study, no significant variations on this parameter have been observed among treatments, suggesting minimal short-term impact of bioplastics residues within the experimental timeframe. Finally, total enzymatic activity, estimated by the fluoresceine hydrolysis assay, was increased in CA+GP mixtures (up to 247 mg fluorescein kg^{-1} h^{-1}), significantly exceeding CTRL and PP. This points to a positive effect of the bioplastics residues in enhancing soil enzymatic activity, which may accelerate organic matter turnover and nutrient cycling, and it is in accordance with recent findings by Song et al. [66], who reported that PLA and PHA enhanced soil nutrient cycling and enzyme activity in an incubation experiment employing cultivated soil.

Overall, these results demonstrate that the presence of CA+GP bioplastics residues can significantly enhance the soil fertility indicators selected after 120 days of incubation. Notably, some positive effects appear to be linked to the persistence of undegraded CA residues, which may function as a semi-recalcitrant C pool contributing to microbial community functioning and soil physical improvements (i.e. CEC, WHC). The observed soil responses reflected short-term microbial and biochemical effects under controlled conditions, while longer-term impacts related to material persistence require further investigation under extended incubation or field conditions.

4. Conclusions

This study demonstrates that the development of sustainable mulch films relies on a strategic balance between material durability and environmental integration. By adopting a *design-by-degradation* approach, we have shown that Cellulose Acetate (CA) and grape pomace (GP) composites can be engineered to synchronize their functional lifespan with the agricultural cycle, providing a reliable alternative to conventional plastics. The experimental results identified the CA+30% GP formulation as the technical optimum for field applications. At this loading, the composite ensures a necessary mechanical tenacity (10.9 MPa) and a stable surface wettability, meeting the industrial requirements for mechanical installation and effective soil protection. Higher filler concentrations (50 wt%), despite accelerating biodegradation, lead to a critical loss of material continuity and excessive brittleness, making them unsuitable for the physical stresses of the mulching process. The integration of FT-IR and thermal data confirms that the

material undergoes a "programmable" failure mechanism. The process begins with plasticizer leaching and enzymatic deacetylation, which act as triggers for the subsequent mechanical collapse of the cellulose backbone. This sequential degradation ensures that the film remains intact during the service life before transitioning into a beneficial soil input. Agronomically, the residues do not act as pollutants; instead, they significantly enhance soil health by increasing total organic carbon (+42%) and stimulating microbial enzymatic activity in the short-term frame analyzed. In conclusion, the CA+30%GP bioplastic composite system represents a mature, circular solution for modern agriculture. By balancing the accelerated decay induced by the filler with the structural integrity required for the application, this work offers a scalable model for producing bio-based materials that may improve soil fertility while adhering to rigorous engineering standards.

Funding sources

This work was supported by the National Recovery and Resilience Plan (NRRP), Mission 4 Component 2 Investment 1.3 - Call for tender No 341 of 15 March 2022 of Italian Ministry of University and Research funded by the European Union – NextGenerationEU Project code PE00000003, Concession Decree No 1550 of 11 October 2022 adopted by the Italian Ministry of University and Research, CUP D93C22000890001, Project title "ON Foods - Research and innovation network on food and nutrition Sustainability, Safety and Security – Working ON Foods".

CRediT authorship contribution statement

Nello Russo: Investigation, Formal analysis, Data curation. **Mirko Cucina:** Writing – review & editing, Investigation, Data curation. **Maria Oliviero:** Writing – review & editing, Investigation, Data curation. **Lucio Pisano:** Investigation, Data curation. **Piero Manna:** Validation, Supervision. **Eugenia Monaco:** Supervision, Funding acquisition.

Declaration of competing interest

The authors declare the following financial interests/personal relationships which may be considered as potential competing interests: Eugenia Monaco reports financial support was provided by Italian Ministry of Universities and Research (MUR).

Data availability

Data will be made available on request.

References

[1] K. Salama, M. Geyer, Plastic mulch films in agriculture: their use, environmental problems, recycling and alternatives, Environments 10 (2023) 179, https://doi.org/10.3390/environments10100179.
[2] A.A. de Souza Machado, W. Kloas, C. Zarfl, S. Hempel, M.C. Rillig, Microplastics as an emerging threat to terrestrial ecosystems, Glob. Chang. Biol. 24 (2018) 1405–1416, https://doi.org/10.1111/gcb.14020.
[3] L. Yang, Y. Zhang, S. Kang, Z. Wang, C. Wu, Microplastics in soil: a review on methods, occurrence, sources, and potential risk, Sci. Tot. Environ. 780 (2021) 146546, https://doi.org/10.1016/j.scitotenv.2021.146546.
[4] P. Tziourrou, J. Bethanis, D. Alexiadis, E. Triantafyllidou, S.G. Papadimou, E. Barbieri, E.E. Golia, Impact of biodegradable plastics on soil health: influence of global warming and vice versa, Microplastics 4 (2025) 43, https://doi.org/10.3390/microplastics4030043.
[5] A. Burato, D. Fichera, S. Cornali, R. Reggiani, D. Ronga, Soil-biodegradable mulching films improve yield, water productivity, and profitability in organic processing tomato, Ital. J. Agron. 20 (2025) 100035, https://doi.org/10.1016/j.ijagro.2025.100035.
[6] A. Weltmeyer, M. Roß-Nickoll, Different mulch films, consistent results: soil fauna responses to microplastic, Environ. Monit. Assess. 196 (2024) 943, https://doi.org/10.1007/s10661-024-13096-x.
[7] M. Zhang, Y. Xue, T. Jin, K. Zhang, Z. Li, C. Sun, Q. Mi, Q. Li, Effect of long-term biodegradable film mulch on soil physicochemical and microbial properties, Toxics 10 (2022) 129, https://doi.org/10.3390/toxics10030129.
[8] Z. Steinmetz, C. Wollmann, M. Schaefer, C. Buchmann, J. David, J. Tröger, K. Muñoz, O. Frör, G.E. Schaumann, Plastic mulching in agriculture. Trading short-term agronomic benefits for long-term soil degradation? Sci. Tot. Environ. 550 (2016) 690–705, https://doi.org/10.1016/j.scitotenv.2016.01.153.
[9] M. Cucina, P. de Nisi, F. Tambone, F. Adani, The role of waste management in reducing bioplastics' leakage into the environment: a review, Bioresour. Technol. 337 (2021) 125459, https://doi.org/10.1016/j.biortech.2021.125459.
[10] E.M.N. Polman, G.-J.M. Gruter, J.R. Parsons, A. Tietema, Comparison of the aerobic biodegradation of biopolymers and the corresponding bioplastics: a review, Sci. Tot. Environ. 753 (2021) 141953, https://doi.org/10.1016/j.scitotenv.2020.141953.
[11] A. Chamas, H. Moon, J. Zheng, Y. Qiu, T. Tabassum, J.H. Jang, M. Abu-Omar, S. L. Scott, S. Suh, Degradation rates of plastics in the environment, ACS Sustain. Chem. Eng. 8 (2020) 3494–3511, https://doi.org/10.1021/acssuschemeng.9b06635.
[12] C. Campanale, S. Galafassi, F. Di Pippo, I. Pojar, C. Massarelli, V.F. Uricchio, A critical review of biodegradable plastic mulch films in agriculture: definitions, scientific background and potential impacts, TrAC Trend. Anal. Chem. 170 (2024) 117391, https://doi.org/10.1016/j.trac.2023.117391.
[13] X. Gao, D. Xie, C. Yang, Effects of a PLA/PBAT biodegradable film mulch as a replacement of polyethylene film and their residues on crop and soil environment, Agric. Water Manag. 255 (2021) 107053, https://doi.org/10.1016/j.agwat.2021.107053.
[14] Y. Guan, F. Cheng, J. Tao, Recent advances in cellulose acetate-based materials, J. Bioresour. Bioprod. 5 (2020) 1–15, https://doi.org/10.1016/j.jobab.2020.03.001.
[15] A. Yadav, K. Behera, Y.H. Chang, F.C. Chiu, Cellulose acetate-based sustainable films for agricultural applications, Carbohydr. Polym. 261 (2021) 117871, https://doi.org/10.1016/j.carbpol.2021.117871.
[16] K.J. Edgar, C.M. Buchanan, J.S. Debenham, P.A. Rundquist, S.T. Seiler, M. C. Shelton, D. Tindall, Advances in cellulose ester performance and application, Prog. Polym. Sci. 26 (2001) 1605–1688, https://doi.org/10.1016/S0079-6700(01)00027-2.
[17] K. Kamide, Cellulose and Cellulose Derivatives, Elsevier Science, Amsterdam, 2005, https://doi.org/10.1016/B978-044451704-3/50001-3.
[18] A.K. Mohanty, M. Misra, L.T. Drzal, Sustainable bio-composites from renewable resources: opportunities and challenges in the green 21st century, J. Polym. Environ. 11 (2003) 19–26, https://doi.org/10.1023/A:1023804726827.
[19] J. Puls, S.A. Wilson, D. Hölter, Degradation of cellulose acetate-based materials: a review, J. Polym. Environ. 19 (2011) 152–165, https://doi.org/10.1007/s10924-010-0258-0.
[20] G. Gadaleta, S. De Gisi, A. Sorrentino, L. Sorrentino, M. Notarnicola, K. Kuchta, C. Picuno, M. Oliviero, Effect of cellulose-based bioplastics on current LDPE recycling, Materials (Basel) 16 (2023) 4869, https://doi.org/10.3390/ma16134869.
[21] C.M. Buchanan, R.M. Gardner, R.J. Komarek, Cellulose acetate: mechanisms of biodegradation, J. Appl. Polym. Sci. 47 (1993) 1709–1719, https://doi.org/10.1002/app.1993.070471001.
[22] R.J. Komarek, R.M. Gardner, C.M. Buchanan, S. Gedon, Biodegradation of cellulose esters: environmental fate of cellulose acetate, J. Appl. Polym. Sci. 50 (1993) 1747–1752, https://doi.org/10.1002/app.1993.070501010.
[23] A.S. Ferreira, C. Nunes, A. Castro, P. Ferreira, M.A. Coimbra, Influence of grape pomace extract incorporation on chitosan films properties, Carbohydr. Polym. 113 (2014) 490–499, https://doi.org/10.1016/j.carbpol.2014.07.032.
[24] Q. Deng, Y. Zhao, Physicochemical, nutritional, and antimicrobial properties of wine grape (cv. Merlot) pomace extract-based films, J. Food. Sci. 76 (2011), https://doi.org/10.1111/j.1750-3841.2011.02090.x.
[25] A. Gowman, A. Rodriguez-Uribe, F. Defersha, A.K. Mohanty, M. Misra, Statistical design of sustainable composites from poly(lactic acid) and grape pomace, J. Appl. Polym. Sci. 137 (2020), https://doi.org/10.1002/app.49061.
[26] A. Gowman, T. Wang, A. Rodriguez-Uribe, A.K. Mohanty, M. Misra, Bio-poly (butylene succinate) and its composites with grape pomace: mechanical performance and thermal properties, ACS Omega 3 (2018) 15205–15216, https://doi.org/10.1021/acsomega.8b01675.
[27] F. D'Urso, P. Iaccarino, M. Giordano, M. Oliviero, E. Di Maio, L. Sansone, A preliminary study on 3D printing feedstock derived from cellulose recovered from cigarette butts, Cellulose 31 (2024) 5097–5114, https://doi.org/10.1007/s10570-024-05886-w.
[28] G. Gadaleta, S. De Gisi, C. Picuno, J. Heerenklage, L. Cafiero, M. Oliviero, M. Notarnicola, K. Kuchta, A. Sorrentino, The influence of bio-plastics for food packaging on combined anaerobic digestion and composting treatment of organic municipal waste, Waste Manage 144 (2022) 87–97, https://doi.org/10.1016/j.wasman.2022.03.014.
[29] M. He, J. Nie, G. Ma, Biodegradable mulch films based on cellulose derivatives, Sci. Total Environ. 723 (2020) 137957, https://doi.org/10.1016/j.scitotenv.2020.137957.
[30] S. Nigam, A.K. Das, M.K. Patidar, Synthesis, characterization and biodegradation of bioplastic films produced from parthenium hysterophorus by incorporating a plasticizer (PEG600), Environ. Chall. 5 (2021) 100280, https://doi.org/10.1016/j.envc.2021.100280.
[31] G. Papa, M. Cucina, K. Echchouki, P. De Nisi, F. Adani, Anaerobic digestion of organic waste allows recovering energy and enhancing the subsequent bioplastic degradation in soil, Resour. Conserv. Recycl. 188 (2023) 106694, https://doi.org/10.1016/j.resconrec.2022.106694.
[32] G.R. Caponio, F. Minervini, G. Tamma, G. Gambacorta, M. De Angelis, Promising application of grape pomace and its agri-food valorization: source of bioactive

molecules with beneficial effects, Sustainability 15 (11) (2023) 9075, https://doi.org/10.3390/su15119075.
[33] R.P. Rodrigues, A.M. Sousa, L.M. Gando-Ferreira, M.J. Quina, Grape pomace as a natural source of phenolic compounds: solvent screening and extraction optimization, Molecules 28 (6) (2023) 2715, https://doi.org/10.3390/molecules28062715.
[34] D.J. da Silva, M.M. de Oliveira, S.H. Wang, D.J. Carastan, D.S. Rosa, Designing antimicrobial polypropylene films with grape pomace extract for food packaging, Food Packag. Shelf Life 34 (2022) 100929, https://doi.org/10.1016/j.fpsl.2022.100929.
[35] I. Ebrahimzade, M. Ebrahimi-Nik, A. Rohani, S. Tedesco, Towards monitoring biodegradation of starch-based bioplastic in anaerobic condition: finding a proper kinetic model, Bioresour. Technol. 347 (2022) 126661, https://doi.org/10.1016/j.biortech.2021.126661.
[36] J. Porras-Saavedra, E. Palacios-González, T. Tovar-Benítez, H. Contreras-Lavida, E. P. Houbron, M. Canul-Chan, Development, soil biodegradation, and kinetics evaluation of starch-based bioplastic from Sechium edule and Phaseoulus vulgaris, Waste Biomass Valoriz. 16 (2025) 1353–1367, https://doi.org/10.1007/s12649-024-02734-7.
[37] M. Cucina, L. Massaccesi, M. Garfí, V. Saponaro, A. Muñoz Muñoz, H. Escalante, L. Castro, Application of digestate from low-tech digesters for degraded soil restoration: effects on soil fertility and carbon sequestration, Sci. Tot. Environ. 967 (2025) 178854, https://doi.org/10.1016/j.scitotenv.2025.178854.
[38] M. Cucina, P. De Nisi, L. Trombino, F. Tambone, F. Adani, Degradation of bioplastics in organic waste by mesophilic anaerobic digestion, composting and soil incubation, Waste Manage 134 (2021) 67–77, https://doi.org/10.1016/j.wasman.2021.08.016.
[39] N. Yadav, M. Hakkarainen, Degradable or not? Cellulose acetate as a model for complicated interplay between structure, environment and degradation, Chemosphere 265 (2021) 128731, https://doi.org/10.1016/j.chemosphere.2020.128731.
[40] F. Bilo, S. Pandini, L. Sartore, L.E. Depero, G. Gargiulo, A. Bonassi, S. Federici, E. Bontempi, A sustainable bioplastic obtained from rice straw, J. Clean. Prod. 200 (2018) 357–368, https://doi.org/10.1016/j.jclepro.2018.07.252.
[41] F.-X. Joly, M. Coulis, Comparison of cellulose vs. plastic cigarette filter decomposition under distinct disposal environments, Waste Manage 72 (2018) 349–353, https://doi.org/10.1016/j.wasman.2017.11.023.
[42] A.C. Resurreccion, P. Moldrup, M. Tuller, T.P.A. Ferré, K. Kawamoto, T. Komatsu, L.W. de Jonge, Relationship between specific surface area and the dry end of the water retention curve for soils with varying clay and organic carbon contents, Water Resour. Res. 47 (2011), https://doi.org/10.1029/2010WR010229.
[43] M. Cucina, The mineralization trap: why current standards for biodegradable plastic biodegradation misread the soil carbon cycle, Environ. Sci. Technol. Lett. 13 (2026) 322–323, https://doi.org/10.1021/acs.estlett.6c00045. In press.
[44] T.F. Nelson, R. Baumgartner, M. Jaggi, S.M. Bernasconi, G. Battagliarin, C. Sinkel, M. Sander, Biodegradation of synthetic aliphatic-aromatic polyesters in soils: linking chemical structure to biodegradability, Environ. Sci. Technol. 59 (37) (2025) 19966–19977, https://doi.org/10.1021/acs.est.5c03099.
[45] M. Mazzon, P. Gioacchini, D. Montecchio, S. Rapisarda, C. Ciavatta, C. Marzadori, Biodegradable plastics: effects on functionality and fertility of two different soils, Appl. Soil Ecol. 169 (2022) 104216, https://doi.org/10.1016/j.apsoil.2021.104216.
[46] V. Titone, M. Rapisarda, L. Pulvirenti, E. Napoli, G. Impallomeni, L. Botta, M. C. Mistretta, P. Rizzarelli, Sustainable biocomposites based on Mater-Bi and grape pomace for a circular economy: performance evaluation and degradation in soil, Polym. Degrad. Stab. 231 (2025) 111091, https://doi.org/10.1016/j.polymdegradstab.2024.111091.
[47] J. Zhu, X. Li, C. Huang, L. Chen, L. Li, Structural changes and triacetin migration of starch acetate film contacting with distilled water as food simulant, Carbohydr. Polym. 104 (2014) 1–7, https://doi.org/10.1016/j.carbpol.2013.12.087.
[48] M. Oliviero, E. Lamberti, L. Cafiero, B. Pace, M. Cefola, G. Gorrasi, A. Sambandam, A. Sorrentino, Biodegradable cellulose acetate/layered double-hydroxide composite film for active packaging of fresh food, Mater. Chem. Phys. 310 (2023) 128469, https://doi.org/10.1016/j.matchemphys.2023.128469.
[49] S. Singh, M.L. Maspoch, K. Oksman, Crystallization of triethyl-citrate-plasticized poly(lactic acid) induced by chitin nanocrystals, J. Appl. Polym. Sci. 136 (2019), https://doi.org/10.1002/app.47936.
[50] J. Zhu, X. Li, C. Huang, L. Chen, L. Li, Plasticization effect of triacetin on structure and properties of starch ester film, Carbohydr. Polym. 94 (2013) 874–881, https://doi.org/10.1016/j.carbpol.2013.02.020.
[51] A. Samir, F.H. Ashour, A.A.A. Hakim, M. Bassyouni, Recent advances in biodegradable polymers for sustainable applications, Npj. Mater. Degrad. 6 (2022) 68, https://doi.org/10.1038/s41529-022-00277-7.
[52] T. Sudiarti, D. Wahyuningrum, B. Bundjali, I. Made Arcana, Mechanical strength and ionic conductivity of polymer electrolyte membranes prepared from cellulose acetate-lithium perchlorate, IOP Conf. Ser. Mater. Sci. Eng. 223 (2017) 012052, https://doi.org/10.1088/1757-899X/223/1/012052.
[53] F.J. Tommasini, L.da C. Ferreira, L.G.P. Tienne, V.de O. Aguiar, M.H.P.da Silva, L. F.da M. Rocha, M.de F.V. Marques, Poly (Methyl Methacrylate)-SiC nanocomposites prepared through in situ polymerization, Mater. Res. 21 (2018), https://doi.org/10.1590/1980-5373-mr-2018-0086.
[54] F. Ruggero, R. Gori, C. Lubello, Methodologies to assess biodegradation of bioplastics during aerobic composting and anaerobic digestion: a review, Waste Manage. Res.: J. Sustain. Circ. Econ. 37 (2019) 959–975, https://doi.org/10.1177/0734242X19854127.
[55] M. Julinová, L. Vaňharová, M. Jurča, A. Minařík, P. Duchek, J. Kavečková, D. Rouchalová, P. Skácelík, Effect of different fillers on the biodegradation rate of thermoplastic starch in water and soil environments, J. Polym. Environ. 28 (2020) 566–583, https://doi.org/10.1007/s10924-019-01624-7.
[56] I. Spiridon, K. Leluk, A.M. Resmerita, R.N. Darie, Development and characterization of cellulose acetate composites reinforced with grape pomace, Polym. Compos. 37 (2016) 2434–2441, https://doi.org/10.1002/pc.23428.
[57] D. Briassoulis, An overview on the mechanical design requirements of agricultural biodegradable technologies, Polym. Test 23 (2004) 1–16, https://doi.org/10.1016/S0142-9418(03)00065-2.
[58] G. Scarascia-Mugnozza, E. Schettini, G. Vox, M. Malinconico, B. Immirzi, S. Pagliara, Mechanical properties of biodegradable films for agricultural mulching, Polym. Test 31 (2012) 199–208, https://doi.org/10.1016/j.polymertesting.2011.09.002.
[59] H.S. Yang, H.J. Kim, J. Son, H.J. Park, B.J. Lee, T.S. Hwang, Rice-husk flour filled polypropylene composites; mechanical and morphological properties, Compos. Struct. 63 (2004) 223–231, https://doi.org/10.1016/S0263-8223(03)00173-6.
[60] H.Y. Sintim, M. Flury, Is biodegradable plastic mulch the solution to agriculture's plastic problem? Environ. Sci. Technol. 51 (2017) 1068–1069, https://doi.org/10.1021/acs.est.7b00346.
[61] A. Belyadi, M. Fasihi, M. Entezam, Effect of natural fillers on the hydrophilicity and biodegradation of biopolymers, J. Appl. Polym. Sci. 138 (2021) 50645, https://doi.org/10.1002/app.50645.
[62] F. Touchaleaume, H. Angellier-Coussy, V. Guillard, E. Gastaldi, Performance and environmental impact of biodegradable mulch films: surface properties and soil interaction, Polym. Degrad. Stab. 129 (2016) 63–76, https://doi.org/10.1016/j.polymdegradstab.2016.03.023.
[63] A. Cano-Larrotta, L. Massaccesi, E. Uggetti, M. Cucina, Unveiling amending properties of biosolids from constructed wetland systems: a comparative study, Sci. Tot. Environ. 999 (2025) 180365, https://doi.org/10.1016/j.scitotenv.2025.180365.
[64] S. Celletti, R. Fedeli, M. Ghorbani, S. Loppi, Impact of starch-based bioplastic on growth and biochemical parameters of basil plants, Sci. Tot. Environ. 856 (2023) 159163, https://doi.org/10.1016/j.scitotenv.2022.159163.
[65] T. Sun, Y. Wang, D. Hui, X. Jing, W. Feng, Soil properties rather than climate and ecosystem type control the vertical variations of soil organic carbon, microbial carbon, and microbial quotient, Soil Biol. Biochem. 148 (2020) 107905, https://doi.org/10.1016/j.soilbio.2020.107905.
[66] D. Song, G. Jin, Z. Su, C. Ge, H. Fan, H. Yao, Influence of biodegradable microplastics on soil carbon cycling: insights from soil respiration, enzyme activity, carbon use efficiency and microbial community, Environ. Res. 266 (2025) 120558, https://doi.org/10.1016/j.envres.2024.120558.